Physics Letters B 750 (2015) 176–180

Contents lists available at ScienceDirect

Physics Letters B

www.elsevier.com/locate/physletb

Evidence for Increased neutron and proton excitations between $^{51-63}$Mn

C. Babcock [a,b,*], H. Heylen [c,**], J. Billowes [d], M.L. Bissell [c], K. Blaum [e], P. Campbell [d], B. Cheal [a], R.F. Garcia Ruiz [c], C. Geppert [f,i], W. Gins [c], M. Kowalska [b], K. Kreim [e], S.M. Lenzi [g], I.D. Moore [h], R. Neugart [e,f], G. Neyens [c], W. Nörtershäuser [i], J. Papuga [c], D.T. Yordanov [e]

[a] Oliver Lodge Laboratory, Oxford Street, University of Liverpool, L69 7ZE, UK
[b] ISOLDE, CERN, CH-1211 Geneva 23, Switzerland
[c] KU Leuven, Instituut voor Kern- en Stralingsfysica, 3001 Leuven, Belgium
[d] School of Physics and Astronomy, University of Manchester, M13 9PL, UK
[e] Max-Planck-Institut für Kernphysik, D-69117 Heidelberg, Germany
[f] Institut für Kernchemie, Johannes Gutenberg-Universität Mainz, D-55128, Germany
[g] Dipartimento di Fisica e Astronomia dell'Università and INFN, Sezione di Padova, I-35131 Padova, Italy
[h] Department of Physics, University of Jyväskylä, PB 35 (YFL) Jyväskylä, Finland
[i] Institut für Kernphysik, TU Darmstadt, D-64289 Darmstadt, Germany

ARTICLE INFO

Article history:
Received 3 July 2015
Received in revised form 12 August 2015
Accepted 5 September 2015
Available online 10 September 2015
Editor: V. Metag

Keywords:
Magnetic dipole moment
Manganese
Spin determination

ABSTRACT

The hyperfine structures of the odd-even $^{51-63}$Mn atoms ($N = 26 - 38$) were measured using bunched beam collinear laser spectroscopy at ISOLDE, CERN. The extracted spins and magnetic dipole moments have been compared to large-scale shell-model calculations using different model spaces and effective interactions. In the case of ^{61,63}Mn, the results show the increasing importance of neutron excitations across the $N = 40$ subshell closure, and of proton excitations across the $Z = 28$ shell gap. These measurements provide the first direct proof that proton and neutron excitations across shell gaps are playing an important role in the ground state wave functions of the neutron-rich Mn isotopes.

© 2015 The Authors. Published by Elsevier B.V. This is an open access article under the CC BY license (http://creativecommons.org/licenses/by/4.0/). Funded by SCOAP[3].

1. Introduction

The complexity of nuclear interactions has made it difficult to define a single model that describes the variety of nuclear properties observed. The nuclear-shell model has been successful in characterizing many of these properties, however predicting phenomena such as the migration of single-particle levels and the disappearance of magic numbers has proven challenging due to the large model spaces needed. Comparisons of shell-model calculations with experimental results, such as electric and magnetic properties, provide a powerful tool to understand nuclear structure evolution and improve its description within the shell model.

Collinear laser spectroscopy is a technique that is used to measure the atomic hyperfine structure, resulting from the interplay between the nucleus and the magnetic and electric fields generated by the electrons. The HFS spectrum allows the magnetic dipole moments and electric quadrupole moments of a nucleus to be derived, as well as a model-independent determination of the nuclear spin [1,2].

Neutron-rich manganese isotopes ($Z = 25$) provide an opportunity for studying shell structure evolution towards the suspected subshell closure at $N = 40$ [3,4]. This appears as a possible subshell closure for ^{68}Ni, observed through a low quadrupole transition probability and a high lying 2_1^+ state [5], however mass measurements of neutron-rich Ni indicate that the closure is a weak one [6]. An increase in collectivity and deformation measured for Fe and Cr in this region [7,8], as well as a lack of significant discontinuities in the 2-neutron separation energies for Fe [9] and Mn [10], also suggests that $N = 40$ is a very weak subshell gap, which decreases quickly as protons are removed from the $1f_{7/2}$ shell. For elements above $Z = 28$, such as Cu and Ga, no magicity is suggested for $N = 40$ from mass measurements [11]. Though the

* Primary corresponding author at: ISOLDE, CERN, CH-1211 Geneva 23, Switzerland.
** Corresponding author.
E-mail addresses: cbabcock@cern.ch (C. Babcock), hanne.heylen@fys.kuleuven.be (H. Heylen).

http://dx.doi.org/10.1016/j.physletb.2015.09.012
0370-2693/© 2015 The Authors. Published by Elsevier B.V. This is an open access article under the CC BY license (http://creativecommons.org/licenses/by/4.0/). Funded by SCOAP[3].

measured nuclear moments of Cu could be interpreted as having a shell gap at $N = 40$, the parity change between the pf and g orbitals could also explain this behavior [12]. In Ga isotopes, strong shape changes have been observed from $N = 40$ to $N = 50$ [13].

Theory suggests that the weakening of the $N = 40$ subshell gap results from the reduction of the proton–neutron interaction as protons are removed from the $1f_{7/2}$ orbital. This results in a reduced binding of the $\nu 1f_{5/2}$ level, and an increased binding of the $\nu 1g_{9/2}$ and $\nu 2d_{5/2}$ levels, thus a reduction of the $N = 40$ gap [8,14]. This is supported by the results of deep-inelastic reaction studies which show that the excited states in heavier odd–odd Mn isotopes occur at energies similar to those of the intruder $\nu 1g_{9/2}$ isomers in the Fe isotones [15].

As a result, quadrupole correlations are enhanced by the excitation of neutrons from the $\nu p_{1/2}$ and $\nu f_{5/2}$ orbitals into the $\nu g_{9/2}$ and $\nu d_{5/2}$ orbitals, making collectivity energetically favorable in these nuclei. The development of quadrupole collectivity also favors the excitation of protons across the $Z = 28$ gap.

This has been observed in the odd Co isotopes at $N = 40$, where ^{67}Co is suggested to have a low lying $1/2^-$ isomer resulting from a proton intruder state coexisting with the ground state [16,17]. In the Mn isotopes, the effect of these proton excitations may be observed in the magnetic moments of the odd-Z ground states.

There have been theoretical attempts to describe this region of the nuclear chart using a variety of effective shell-model interactions, one of the most used being the GXPF1A interaction, which models the full pf space [18,19]. This interaction has been very successful in describing nuclei with particles in the mid-pf shell, however for isotopes approaching $N = 40$, the exclusion of the $\nu 1g_{9/2}$ orbital from the model space limits its effectiveness [4,20]. The model space has therefore been extended to the $pfg_{9/2}$ orbitals and the isotopes $^{57-63}$Mn have been investigated with various interactions [4,21]. Good agreement with published excitation energy data has been found for most of the isotopes, but information on the electromagnetic properties is required to fully test the interactions. In order to reproduce the observed quadrupole collectivity, it has been argued that it is also necessary to take into account the $\nu 2d_{5/2}$ level [22]. This has been incorporated into the LNPS interaction [22], using a ^{48}Ca core and allowing excitations to $\nu 1g_{9/2}$ and $\nu 2d_{5/2}$. It greatly expands the computational domain as compared to the previously discussed models, and has been used successfully to describe energies and transition probabilities in the elements Fe [3,23], Cr [8,24], Co [17] and Cu [25].

In view of the theoretical challenges, and the need for data to better characterize the nuclear structure changes and test the effective nucleon–nucleon interactions in this region, we present here measurements of the spins, A and B hyperfine coefficients, and the deduced magnetic dipole moments of the odd isotopes in $^{51-63}$Mn, as well as a comparison with theory.

2. Experimental setup

Manganese ions were produced by the impact of a 1.4-GeV proton beam produced by the PS Booster at CERN on a thick uranium carbide target. The yield of Mn ions was increased, and isobaric contaminants minimized, through the use of ISOLDE's resonant laser ion source (RILIS) [26]. After passage through a mass separator, the ions were trapped in a radio-frequency quadrupole cooler and buncher [27] for approximately 50 ms before being released in 6 μs bunches to the collinear laser spectroscopy beamline (COLLAPS, see [28]).

At the COLLAPS setup, the ion beam entered a charge-exchange cell filled with sodium vapor which was floating on the Doppler tuning potential. The ion beam emerged from the charge-exchange cell as an atomic beam and was overlapped with a co-propagating COLLAPS laser used to probe the transition of interest. Up to four photomultiplier tubes positioned around the interaction region detected the emitted fluorescence. Background suppression was accomplished by gating the photomultipliers to accept only photons which arrived during the time the atom bunch was traversing the interaction region, thus reducing the background due to randomly scattered photons and dark counts by a factor of approximately 10^4 [1]. The atomic transition from the $3d^5\,4s^2\ ^6S_{5/2}$ (ground state) to the $3d^5\,4s4p\ ^6P_{3/2}$ excited state at 35 689.98 cm^{-1} was probed using a narrow band dye laser providing approximately 1–3 mW of light at 280.2 nm. The 40 keV ion beam energy was tuned using the potential of the charge-exchange cell, so that the laser frequency (as seen by the fast atom beam) was Doppler shifted over the range corresponding to the hyperfine splitting.

Fitting the spectra with a least-squares minimization procedure and Lorentzian profiles yields the hyperfine structure coefficients A and B, for the upper and lower states, as well as the nuclear spins. Because of the low laser power density, the relative intensities of the hyperfine structure components were fixed to the Racah intensities to further constrain the fit.

In the fitting routine, parameters to describe the multi-component resonance profile were included. Processes such as collisional excitation and non-resonant charge-exchange result in the formation of some atoms in an excited state, the energy for which is transferred from the kinetic energy of the beam. When these excited atoms decay back to the atomic ground state, they require a higher acceleration voltage to reach the Doppler-shifted resonance frequency. The additional peaks produced by these atoms are located at a slightly lower frequency, very close to the main resonance peak [29]. This was taken into account in the fitting procedure by the inclusion of a second Lorentzian profile associated with each line. Each of these secondary peaks was given a fixed energy offset of 4.43 eV, corresponding to the energy of the populated state (determined through the fit of the high-statistics ^{55}Mn data), and a fitted relative intensity. The fits to the relative intensities indicate that the atoms affected by these inelastic processes during charge-exchange constitute approximately 20% of the total measured beam.

In the case of ^{63}Mn, which has a shorter half life than the other isotopes (250 ms), a proton triggering technique was used which consists of accepting photons only during a time window after each proton impact corresponding to one half life of the isotope. This enhanced the signal to noise ratio on the observed hyperfine structure by further suppressing the stray light background.

3. Results

Table 1 shows the hyperfine coefficients A and B of the upper state. Literature values for the coefficients of the lower state of ^{55}Mn are $A_l = -72.420836(15)$ MHz and $B_l = -0.019031(17)$ MHz, obtained in spin-exchange optical pumping experiments [30]. Good agreement is shown between the A_l value from this work ($A_l = -72.4(7)$ MHz) and the literature value. In this analysis, the ratio A_l/A_u was constrained to be 0.0752, as determined from the high statistics data for ^{55}Mn. A negligible hyperfine anomaly is assumed at this level of accuracy. The A values have been used to calculate the magnetic moments of the isotopes using [1],

$$\mu = \mu_{\mathrm{ref}} \frac{I\,A}{I_{\mathrm{ref}}\,A_{\mathrm{ref}}}$$

with the value of $\mu_{\mathrm{ref}} = +3.46871790(9)$ taken from [31]. Since the value of B_l is much less than 1 MHz, it has been constrained to zero. Sensitivity to the quadrupole moment in the upper state is also very weak, resulting in a large relative uncertainty for

Table 1
The measured nuclear spins, and A and B hyperfine coefficients for the $^6P_{3/2}$ excited state. Magnetic dipole moments are determined as described in Section 3. Values are compared to shell-model calculations using the GXPF1A and the LNPS effective interactions with free nuclear g-factors. All moments are given in units of μ_N.

Isotope	A (MHz)	B (MHz)	Spin	μ	μ [GXPF1A]	μ [LNPS]
^{51}Mn	−993.7(12)	17(9)	5/2	+3.577(4)	+3.46	–
^{53}Mn	−996.8(8)	3(8)	7/2	+5.024(4)	+4.76	–
^{55}Mn	−963.1(3)	14(1)	5/2	–	+3.35	–
^{57}Mn	−967.4(5)	9(4)	5/2	+3.483(2)	+3.44	+3.60
^{59}Mn	−970.3(5)	7(4)	5/2	+3.493(2)	+3.48	+3.56
^{61}Mn	−981.6(4)	16(3)	5/2	+3.534(1)	+3.62	+3.56
^{63}Mn	−954.3(11)	10(8)	5/2	+3.435(4)	+3.77	+3.48

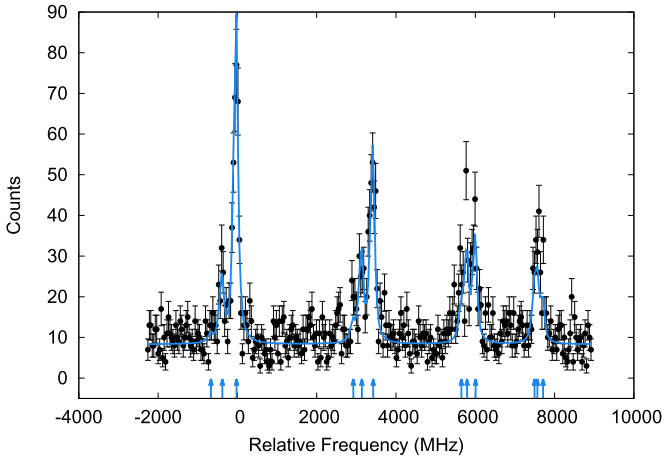

Fig. 1. HFS data from ^{63}Mn with fit for spin 5/2 overlaid, frequencies shown relative to the ^{55}Mn center of gravity. The arrows indicate the predicted positions of the peaks (color online).

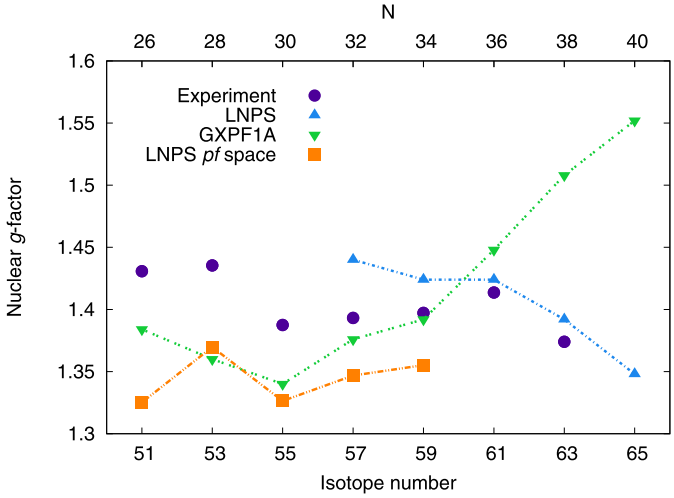

Fig. 2. Comparison of experimental data from this study to calculations using the GXPF1A interaction, the LNPS interaction, and the LNPS interaction in the pf shell but instead using a ^{40}Ca core and blocking excitations to the neutron $g_{9/2}$ and $d_{5/2}$ orbitals. All calculations were performed with free g-factors. Error bars are within the symbols (color online).

B_u, therefore quadrupole moments have not been extracted. Spectroscopy on the isotopes $^{50-56}$Mn has already been described and compiled elsewhere [30–32], and the reported magnetic moments for ^{51,53}Mn are in agreement with our results.

An advantage of laser spectroscopy is the possibility of making an unambiguous determination of nuclear spins. The spins of all odd–even isotopes for $A = 51 - 63$ have been measured here by analyzing the pattern of the HFS peaks, as shown in Fig. 1.

Table 1 shows the spin values derived from the least-squares fit to the spectra. Where uncertainties existed, the spin was confirmed by the observation that the use of an alternative value for the spin in the fitting procedure produces a B coefficient that is unphysically large. For example, assuming $I = 7/2$ for ^{63}Mn gives $B = -229(8)$ MHz which would yield the unrealistically large quadrupole moment $Q_s = -5.8(9)$ b. For ^{59}Mn and ^{61}Mn, the quadrupole moments would be similarly large, $Q_{s,59} = -5.9(9)$ b and $Q_{s,61} = -5.6(8)$ b.

In an independent particle shell-model interpretation, the odd manganese isotopes with 3 holes in the $\pi f_{7/2}$ shell would have a spin 7/2 ground state. However, except for ^{53}Mn (with 28 neutrons), all isotopes have been found to have spin 5/2.

4. Discussion

Shell-model calculations of the energy levels and moments of neutron-rich isotopes in the region $Z = 20$ to $Z = 28$ have sought to characterize the rapid structure evolution and lack of a robust sub-shell closure near $N = 40$. Using the code ANTOINE [33] and the GXPF1A effective interaction [19], calculations of the magnetic moments of neutron-rich Mn have been performed in the pf model space, allowing up to eight particles (maximum 2 protons and 6 neutrons) to be excited from the $1f_{7/2}$ to the $2p_{3/2}$, $1f_{5/2}$ and $2p_{1/2}$ orbitals.

Magnetic moments and their associated g-factors are highly sensitive to the nuclear wave function, and provide a stringent test of the models. Shell-model results obtained with free g-factors ($g = \mu_I / I\,\mu_N$) are shown in Fig. 2 and compared to the experimental results. Calculations using the GXPF1A interaction do not reproduce the observed trend very well, but given the scale, the absolute values are reproduced within a 1–10% range up to ^{61}Mn. Using effective g-factors does not significantly improve the overall agreement. From $N = 36$ onwards, the GXPF1A calculations predict an increase in the g-factors towards the Schmidt value, as would be expected if $N = 40$ were a magic number. Instead, the experimental data shows a decrease after $N = 36$.

The widening discrepancy between the measured magnetic moments and the GXPF1A calculations suggests that the model space is insufficient to describe the structural changes in the heavier isotopes. If the $\nu 1g_{9/2}$ and $\nu 2d_{5/2}$ orbitals play a crucial role, as has been proposed to reproduce the level scheme of ^{66}Fe [3,23] and in Cr [24], then the model space must be expanded. These orbitals are taken into account by the LNPS interaction, which includes the entire pf shell for protons and the levels $1f_{5/2}$, $2p_{3/2}$, $2p_{1/2}$, $1g_{9/2}$ and $2d_{5/2}$ for neutrons [22]. Calculations done with this interaction reproduce very well the decreasing trend in the g-factors from ^{61}Mn ($N = 36$) onwards, as shown in Fig. 2. The calculated free g-factors agree with the observed values for ^{61,63}Mn to within 1%. This confirms the importance of neutron excitations across $N = 40$ for isotopes with neutron numbers $N = 36$ and higher. For the sake of completeness, the results of LNPS calculations for the lighter Mn

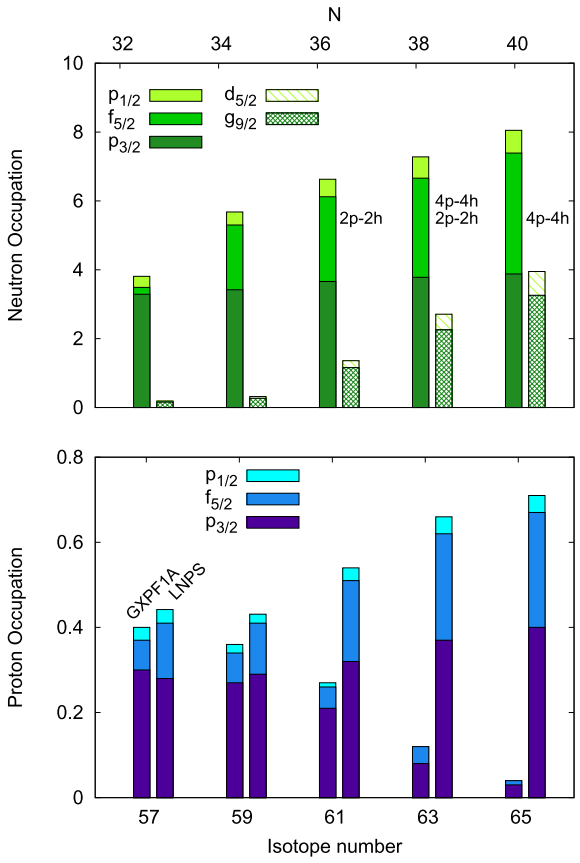

Fig. 3. Top: Orbital occupation numbers for neutrons calculated using the LNPS interaction. Occupation levels are grouped into the pf group ($\nu p_{3/2}$, $\nu f_{5/2}$, $\nu p_{1/2}$) and the gd group ($\nu g_{9/2}$, $\nu d_{5/2}$). Bottom: Orbital occupation numbers for protons excited across $Z = 28$ calculated using the GXPF1A and LNPS interactions (color online).

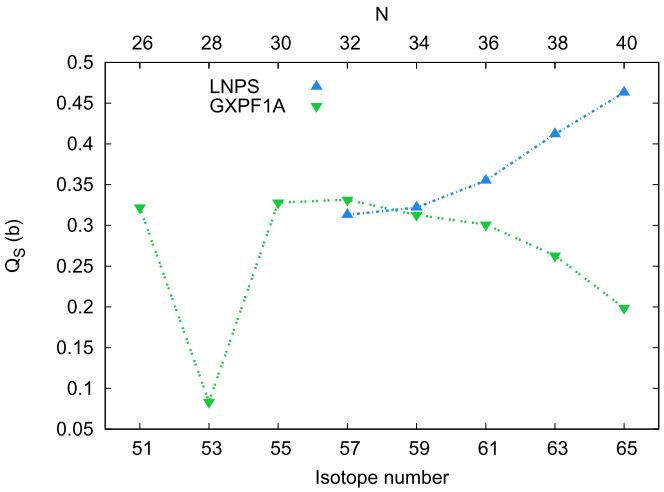

Fig. 4. The electric quadrupole moments as predicted by the GXPF1A and LNPS effective interactions (color online).

isotopes, using the full pf space with a ^{40}Ca core and blocking excitations to the $\nu 1g_{9/2}$ and $\nu 2d_{5/2}$ orbitals are also shown in Fig. 2. As expected, these results are similar to those of GXPF1A.

Since the observed magnetic moments of ^{57,59}Mn are better reproduced by the GXPF1A calculations, and the trend in the heavier isotopes can only be reproduced by the LNPS calculations, these results can be used to investigate changes in the ground state wave functions of odd-A Mn isotopes with increasing neutron number from ^{57}Mn ($N = 32$) onwards. Fig. 3 shows the predicted occupation of the relevant orbitals for the ground state wave function.

As expected, the level occupations calculated with LNPS show that additional neutrons are preferentially excited into the $1g_{9/2}$ orbital, with a marked augmentation of the $2d_{5/2}$ level occupation as well. The LNPS predicted ground state configuration for ^{65}Mn ($N = 40$) is dominated by 4p-4h neutron excitations, as is the case for Fe, Cr, Ti and Ca [22], indicating the strong contribution of these configurations to the wave function.

In the case of the protons, a comparison between the level occupation predicted with the LNPS and GXPF1A interactions shows that LNPS predicts increasing numbers of proton excitations in the upper pf shell while GXPF1A predicts decreasing numbers, and far fewer excited protons in total, as one moves towards $N = 40$. The accuracy of the LNPS interaction in predicting the measured g-factors at higher neutron number, along with the predicted increase in proton excitations across $Z = 28$, suggest that proton excitations play a pivotal role in the structural evolution observed in this mass region. The removal of protons from the $f_{7/2}$ orbital as one moves away from ^{68}Ni induces a stronger binding of the orbits $\nu 1g_{9/2}$ and $\nu 2d_{5/2}$, allowing neutron promotion across $N = 40$. The promotion of these neutrons then results in a repulsive potential with the $\pi 1f_{7/2}$ orbital and an attractive potential with the $\pi 1f_{5/2}$ orbital, contributing to the reduction of the $Z = 28$ shell gap and thus enhancing the probability for the excitation of protons across it. A similar explanation has been put forth to describe the Type-II shell evolution seen in the $0^+_{1,2,3}$ states of ^{68}Ni, calculated using the advanced Monte Carlo shell-model [34], and to describe the level structure in neutron-rich Cu [25]. The resulting increase in deformation is reflected in the ground state spins, shown in Table 1, where spin 5/2 is favored over the expected spin 7/2 [20,35]. The ground state spins are correctly predicted to be 5/2 by both GXPF1A [4,36] and LNPS, with the 7/2 states in ^{57,59,61,63}Mn at less than 300 keV for both interactions.

There are two abrupt decreases in the g-factors visible in Fig. 2, after $N = 28$ and after $N = 36$. The first discontinuity can be explained by the occupation of the higher νpf orbitals beyond $N = 28$, which allows for more proton–neutron correlations. A similar effect was seen in Cu isotopes near $N = 28$ [12,37]. The discontinuity between $N = 36$ and $N = 38$ is induced by the increase in proton occupation of the higher pf orbitals, as shown in the LNPS calculations. The increased occupation of the $\pi f_{5/2}$ orbital from $N = 36$ onwards leads to small admixtures of the spin-orbit partner $\pi 1f_{5/2}$ into the wave function dominated by the $\pi 1f_{7/2}$ configuration, and this has a significant effect on the calculated magnetic moments [38].

As demonstrated, the magnetic moments are sensitive probes of the nuclear wave function and have provided the first evidence for the influence of intruder orbitals on the ground states of isotopes with $N < 40$. However, the magnetic dipole moment is only indirectly sensitive to collectivity, whereas the electric quadrupole moment provides a direct probe of the quadrupole correlations between nucleons. Fig. 4 shows the GXPF1A and LNPS predictions for the quadrupole moments of Mn isotopes, in which the two predictions can be seen to deviate significantly starting at ^{61}Mn. This deviation can be attributed to increased correlations resulting from excitations across $N = 40$ and $Z = 28$, which are only included in the LNPS calculation. In this region of the nuclear chart, where the onset of collectivity has been observed in Fe and Cr [3,39], comparison of experimentally determined quadrupole moments to the GXPF1A and LNPS predictions will provide valuable information on the degree of collectivity in manganese isotopes.

5. Conclusions

Nuclear spins as well as magnetic dipole moments have been reported for the odd–even isotopes $^{51-63}$Mn. The magnetic moments have been compared to shell-model calculations based on the GXPF1A and LNPS interactions. As a result of this comparison, it is found that the neutron $1g_{9/2}$ and $2d_{5/2}$ orbitals are required in the model space in order to reproduce the dipole moments for ^{61}Mn and heavier isotopes. This highlights the importance of neutron excitations, which lead to an increase of proton excitations across the $Z = 28$ shell gap from $N = 36$ onwards. The larger proton population in the higher pf orbitals, as well as the weakening of the $N = 40$ closure in manganese (and other neighboring isotope chains), produce an increase in quadrupole correlations, as shown by the LNPS predicted quadrupole moments. A future measurement of the quadrupole moments of these isotopes, using a laser transition with greater sensitivity to the hyperfine B coefficient, will shed more light on this.

Acknowledgements

This work was supported by the Belgian Research Initiative on Exotic Nuclei (IAP-project P7/12), the FWO-Vlaanderen, GOA grant 10/010 from KU Leuven, BMBF (05 P12 RDCIC), the Max-Planck Society, the Science and Technology Facilities Council, a Marie Curie ITN Fellowship of the European Community's FP7 Programme (PITN-GA-2010-264330-CATHI), and EU FP7 via ENSAR (No. 262010). We would like to thank the ISOLDE technical group for their support and assistance.

References

[1] B. Cheal, K. Flanagan, J. Phys. G, Nucl. Part. Phys. 37 (2010) 113101.
[2] K. Blaum, J. Dilling, W. Nörtershäuser, Phys. Scr. 2013 (2013) 014017.
[3] J. Ljungvall, et al., Phys. Rev. C 81 (2010) 061301.
[4] J.J. Valiente-Dobón, et al., Phys. Rev. C 78 (2008) 024302.
[5] O. Sorlin, et al., Phys. Rev. Lett. 88 (2002) 092501.
[6] S. Rahaman, et al., Eur. Phys. J. A 34 (2007) 5.
[7] O. Sorlin, et al., Eur. Phys. J. A 16 (2003) 55.
[8] H.L. Crawford, et al., Phys. Rev. Lett. 110 (2013) 242701.
[9] R. Ferrer, et al., Phys. Rev. C 81 (2010) 044318.
[10] S. Naimi, et al., Phys. Rev. C 86 (2012) 014325.
[11] C. Guénaut, et al., Phys. Rev. C 75 (2007) 044303.
[12] P. Vingerhoets, et al., Phys. Rev. C 82 (2010) 064311.
[13] B. Cheal, et al., Phys. Rev. Lett. 104 (2010) 252502.
[14] T. Otsuka, et al., Phys. Rev. Lett. 95 (2005) 232502.
[15] C.J. Chiara, et al., Phys. Rev. C 82 (2010) 054313.
[16] D. Pauwels, et al., Phys. Rev. C 78 (2008) 041307.
[17] F. Recchia, et al., Phys. Rev. C 85 (2012) 064305.
[18] M. Honma, T. Otsuka, B.A. Brown, T. Mizusaki, Phys. Rev. C 69 (2004) 034335.
[19] M. Honma, T. Otsuka, B.A. Brown, T. Mizusaki, Eur. Phys. J. A 25 (2005) 499.
[20] D. Radulov, et al., Phys. Rev. C 88 (2013) 014307.
[21] H. Jin, Y. Sun, K. Kaneko, S. Tazaki, Phys. Rev. C 87 (2013) 044327.
[22] S.M. Lenzi, F. Nowacki, A. Poves, K. Sieja, Phys. Rev. C 82 (2010) 054301.
[23] W. Rother, et al., Phys. Rev. Lett. 106 (2011) 022502.
[24] T. Baugher, et al., Phys. Rev. C 86 (2012) 011305.
[25] E. Sahin, et al., Phys. Rev. C 91 (2015) 034302.
[26] B. Marsh, et al., Hyperfine Interact. 196 (2010) 129.
[27] H. Frånberg, et al., Nucl. Instrum. Methods Phys. Res., Sect. B, Beam Interact. Mater. Atoms 266 (2008) 4502.
[28] J. Papuga, et al., Phys. Rev. C 90 (2014) 034321.
[29] K.R. Anton, et al., Phys. Rev. Lett. 40 (1978) 642.
[30] S. Davis, J. Wright, L. Balling, Phys. Rev. A 3 (1971) 1220.
[31] N. Stone, At. Data Nucl. Data Tables 90 (2005) 75.
[32] F. Charlwood, et al., Phys. Lett. B 690 (2010) 346.
[33] E. Caurier, F. Nowacki, Acta Phys. Pol. B 30 (1999) 705.
[34] Y. Tsunoda, et al., Phys. Rev. C 89 (2014) 031301.
[35] J. Comfort, P. Wasielewski, F. Malik, W. Scholz, Nucl. Phys. A 160 (1971) 385.
[36] D. Steppenbeck, et al., Phys. Rev. C 81 (2010) 014305.
[37] T.E. Cocolios, et al., Phys. Rev. Lett. 103 (2009) 102501.
[38] H. Noya, A. Arima, H. Horie, Prog. Theor. Phys. Suppl. 8 (1958) 33.
[39] N. Aoi, et al., in: INPC 2007 Proceedings of the 23rd International Nuclear Physics Conference, Nucl. Phys. A 805 (2008) 400c.